Development and Characterization of Green Fluorescent Protein Mutants with Altered Lifetimes†

Allan W. Scruggs,‡ Carole L. Flores,§ Rebekka Wachter,|| and Neal W. Woodbury*,§

Barrow Neurological Institute, St. Joseph's Hospital and Medical Center, Phoenix, Arizona 85013, Center for Biooptical Nanotechnology, Biodesign Institute at Arizona State University, Tempe, Arizona 85287, and Department of Chemistry and Biochemistry, Arizona State University, Tempe, Arizona 85287-1604

Received March 24, 2005; Revised Manuscript Received August 3, 2005

ABSTRACT: Multiple-probe fluorescence imaging applications demand an ever-increasing number of resolvable probes, and the use of fluorophores with resolvable fluorescence lifetimes can help meet this demand. Green fluorescent protein (GFP) and its variants have been widely used in spectrally resolved multiprobe imaging, but as yet, there has not been a systematic set of mutants generated with resolvable lifetimes. Therefore, to generate such mutants, we have utilized error-prone PCR and fluorescence lifetime imaging to screen for mutants of UV-excited green fluorescent protein (GFPuv) that exhibit altered fluorescence decay lifetimes. This has resulted in the isolation of GFPuv mutants displaying at least three distinctly different lifetimes in the range of 1.9−2.8 ns. Mutation of Y145 to either histidine or cysteine was found to shift the fluorescence lifetime of GFPuv from 3.03 ± 0.03 to 2.78 ± 0.05 ns for the Y145H mutant and to 2.74 ± 0.05 ns for Y145C. Some of the shorter-lifetime mutants exhibited excitation peaks that were red-shifted relative to their maximal absorption, indicating that the mutations allowed the adoption of additional conformations relative to wtGFPuv. The utility of these mutants for applications in simultaneous imaging and quantification is shown by the ability to quantify the composition of binary mixtures in time-resolved images using a single detector channel. The application of the screening method for generating lifetime mutants of other fluorescent proteins is also discussed.

The green fluorescent protein (GFP)[1] from *Aequorea victoria* has been widely used as a marker in molecular biology studies since it was discovered that it could fluoresce in the absence of exogenous cofactors. Spectral mutants of GFP have been extensively used in multiple-probe microscopy, fluorescence resonance energy transfer (FRET) imaging, and fluorescence lifetime imaging microscopy (FLIM) (*1*−*5*). As a result of the increasing number of applications for fluorescence imaging of multiple probes, the demand for the number of separable probes has also increased (*6*). Spectral deconvolution (or linear unmixing) has been used recently to image and separate the signals from four different fluorescent proteins (*3*). However, the limitations of spectral discrimination can place an upper limit on the number of resolvable probes that can be developed by rational or random mutagenesis techniques.

Fluorescent proteins such as GFP and its mutants can be distinguished not only on the basis of their spectral differences but also on the basis of their difference in fluorescence decay lifetimes. Multiple-probe imaging using lifetime-based discrimination of fluorescent proteins has been reported previously (*5*). Lifetime imaging is also very useful in detecting fluorescence resonance energy transfer (FRET), in which case the lifetime of the donor is monitored for the characteristic decrease upon quenching by the acceptor fluorophore. The ability to take time-resolved measurements of GFP fluorescence opens a new possible avenue for the creation of additional fluorescent proteins that can be distinguished on the basis of their fluorescence lifetime. Such proteins would have the advantages of GFP, including the ability to tag and track endogenous protein expression within living cells, and would maintain the spectral properties of the fluorescent protein from which they are derived. The wide use of time-correlated single-photon counting methods in imaging applications allows the fluorescence decay profile at each pixel to be determined in a single imaging scan (*1*). Thus, using fluorescent proteins with similar excitation and emission profiles but different fluorescence lifetimes can allow multiple probes to be differentiated in an image in a single-channel detection experiment, with minimal photodamage to either the organism or the probe.

The lifetime of wtGFP has been measured to be ∼3.1 ns; enhanced GFP exhibits an excitation wavelength-dependent lifetime ranging from 2.7 to 3.4 ns, and enhanced cyan

† This work was funded by NSF IGERT (DGE-0114434), NSF Grants BES-0086920,001 and MCB0131776, and USDA Grant 20013531810931.

* To whom correspondence should be addressed: Department of Chemistry and Biochemistry, Arizona State University, Tempe, AZ 85287-1604. Telephone: (480) 965-3294. Fax: (480) 965-2747. E-mail: NWoodbury@asu.edu.

‡ St. Joseph's Hospital and Medical Center.

§ Biodesign Institute at Arizona State University.

|| Department of Chemistry and Biochemistry, Arizona State University.

[1] Abbreviations: GFP, green fluorescent protein; GFPuv, UV-excited green fluorescent protein; FRET, fluorescence resonance energy transfer; FLIM, fluorescence lifetime imaging microscopy; ECFP, enhanced cyan fluorescent protein; pGFPuv, plasmid DNA containing the GFPuv gene; PMT, photomultiplier tube; wtGFPuv, wild-type GFPuv; EGFP, enhanced GFP; CFP, cyan fluorescent protein; YFP, yellow fluorescent protein; EYFP, enhanced YFP; BFP, blue fluorescent protein.

10.1021/bi050550f CCC: $30.25
Published on Web 09/16/2005

fluorescent protein (ECFP) has a lifetime of ~3.6 ns (*7*, *8*). However, it is not obvious from the information available on GFP how to best engineer a protein that maintains the spectral properties of GFP, yet has a significantly altered fluorescence lifetime. Directed evolution techniques have been previously applied to GFP to select for specific spectral qualities or for emission which depends on the presence of a particular analyte (*9*, *10*). Here, directed evolution methods are applied in combination with lifetime imaging of GFPuv (a UV-excited GFP variant, described in ref *9*) to generate GFPuv mutants with altered fluorescence lifetimes, while leaving the spectral properties of GFPuv unchanged. In this way, a wide range of lifetimes could be generated, in a relatively quick and generally applicable way without a priori knowledge of the required mutations.

MATERIALS AND METHODS

Strains and Plasmids. Plasmid DNA containing the GFPuv gene (pGFPuv) was purchased from Clontech (Palo Alto, CA). Error-prone PCR was used to create the first-generation libraries using previously described methods (*11*). The primers used were 5′ACAGCTATGACCATGATTACG3′ (forward) and 5′CATTACCAACTTGTCTGGTGT3′ (reverse). PCR amplification of the desired region was checked by gel electrophoresis, and the amplification product was subjected to DpnI digestion to remove parental DNA from the mixture. Amplified, undigested product was purified by the use of the MinElute PCR Purification (Qiagen, Valencia, CA) system according to the manufacturer's protocol, digested with HindIII and EcoRI, and again purified using the MinElute kit.

Empty backbone vector (pGFPuv with the GFPuv coding region excised) was ligated to the digested PCR product using T4 DNA ligase. The ligated, randomly mutated pGFPuv was electroporated into DH10B electrocompetent cells (Invitrogen) using a Bio-Rad MicroPulser after which 100 μL of cells (from a total volume of 1 mL) was plated on Luria broth (~10^3 colonies; thus, the total library size was ~10^4) and incubated overnight at 37 °C. The remainder of the transformed cells were stored at −80 °C. Sequencing of selected mutants verified an error rate of 0.3% (two to three changes per gene).

Fluorescence Lifetime Imaging and Selection. The apparatus used to screen libraries of mutant pGFPuv colonies is shown in Figure 1. A titanium:sapphire laser (Spectra-Physics, Mountain View, CA) tuned to 800 nm with a 100 fs pulse width and an 82 MHz repetition rate generated 1.8 W of output. This beam was directed through an electrooptic modulator (Conoptics, Danbury, CT) and into a frequency doubler, which generated 400 mW of 400 nm light. This was reflected by a dichroic mirror (Omega Optical, Brattleboro, VT) into an XY-plane scan head (Nutfield Technology, Windham, NH), which moved the beam over the surface of the plate, located approximately 9 in. from the focusing lens of the scan head. The fluorescence from GFPuv was collected by the scan head lens and mirrors and passed through the dichroic mirror and a 520 nm band-pass filter with a 40 nm pass band (Omega Optical) to a PMH-100 photomultiplier tube (PMT, Becker-Hickl, Berlin, Germany). Fluorescence data were sent to a Becker and Hickl SPC-830 card recording in "scan-sync in" mode using an external pixel clock

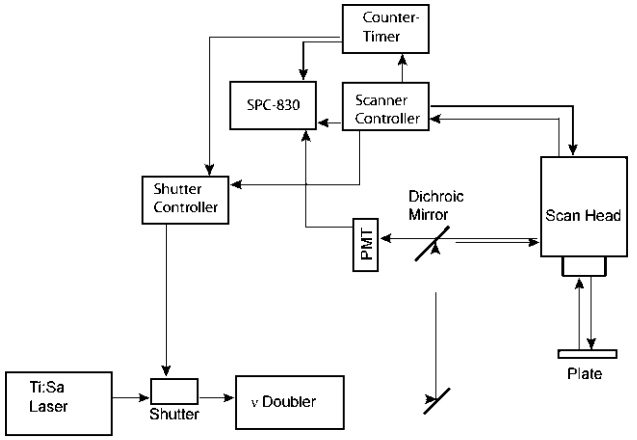

FIGURE 1: Schematic of the scanning laser system. Fluorescence excitation of the sample is achieved by scanning 400 nm laser light over the surface of the plate, and fluorescence is collected through the dichroic mirror by the photomultiplier tube. Signals are analyzed using a Becker and Hickl SPC-830 card.

generated by a National Instruments (Austin, TX) PCI-6014 counter/timer board using line-start output from the scan head. Images collected were 256 × 256 pixels with 256 time bins containing the time-correlated single-photon counting histograms for each image pixel. Images were then analyzed using MATLAB algorithms by first calculating pixel intensity, defined as the sum of the photons in all time bins in a particular pixel. An intensity histogram of each image was used to determine a fluorescence threshold value; pixels with intensities higher than this value were further analyzed for fluorescence lifetime. Fluorescent colonies were defined as each set of connected pixels with intensities above the fluorescence threshold value. Decay curves for each pixel in a colony were summed together, allowing for a higher signal-to-noise ratio. Lifetimes were then calculated by normalizing each decay curve to its maximum and using nonlinear least-squares curve fitting to the function

$$I = Ae^{(-t/\tau)} + c \quad (1)$$

where I represents the normalized intensity, A is a pre-exponential factor, τ is the fluorescence decay time in nanoseconds, and c represents the uncorrelated background signal. The initial values that were passed to the fitting function were as follows: $A = 1.0$, $\tau = 3.0$ ns, and $c = 0.001$. A scatter plot of the lifetimes of all colonies in the image versus their intensity was made, and colonies significantly deviating from the bulk of the colonies were manually picked off of the plate and used to inoculate 3 mL of LB and 50 μg/mL ampicillin. These liquid cultures were incubated at 37 °C overnight with shaking, after which they were diluted 1:10^5, and 100 μL was plated on LB/50 μg/mL ampicillin plates. After incubation of the plate at 37 °C overnight, the plate was imaged again and analyzed for lifetimes. A single colony displaying the expected fluorescence lifetime (the lifetime determined in the original screening) was selected from the plate to inoculate 3 mL of LB and 50 μg/mL ampicillin, which was incubated overnight and supplemented with glycerol for storage at −80 °C. If no such colony was found, the plate was discarded.

Sequencing and Subsequent Mutagenesis. Freezer stocks of each isolated mutant from a particular generation were

streaked on LB/50 μg/mL ampicillin plates, and single colonies from each streak were used to inoculate 5 mL liquid overnight cultures. Cells were harvested by centrifugation in a microcentrifuge at the maximum speed for 30 s, and plasmid DNA from each mutant was isolated using the Qiagen Plasmid MiniPrep kit (Qiagen). DNA concentrations were determined by measuring the optical absorbance at 260 nm on a Cary 50 spectrophotometer (Varian, Palo Alto, CA). Approximately 300 ng of plasmid from each mutant was sent for sequencing to the Arizona State University sequencing facility. For creation of the succeeding generations, DNA from each mutant in a generation was combined in equal amounts to yield 100 ng of total plasmid DNA, and this was subjected to mutagenic PCR and transformed; the resultant colonies were screened as described above.

Mutant Characterization. To prepare wtGFPuv and all mutant proteins from cells for spectral analysis, 5 mL liquid cultures in LB and 50 μg/mL ampicillin were inoculated from streaked plates and incubated overnight at 37 °C in loosely capped tubes with shaking to promote the oxygen-mediated chromophore formation of GFPuv. Cells were harvested by centrifugation in a microcentrifuge and resuspended in 0.5 mL of 0.02 M Tris-HCl (pH 8.0). These samples were then frozen at −80 °C for >1 h and then thawed, vortexed, and centrifuged for 10 min at 13 000 rpm in a microcentrifuge to remove cellular debris. The supernatant containing soluble GFPuv was concentrated to 100 μL using MicroCon 50 kDa centrifugal filters (Millipore, Billerica, MA) and stored at 4 °C. Absorbance spectra were collected on a Cary 50 spectrophotometer (Varian) by placing the entire 100 μL volume of each sample in a quartz microcuvette and recording the absorbance spectrum between 225 and 600 nm, using 100 μL of 0.02 M Tris-HCl (pH 8.0) as a baseline. Samples were removed from the cuvette by pipetting and stored at 4 °C for later use. Fluorescence emission and excitation spectra were recorded using a home-built fluorimeter (*12*) by diluting each sample 1:20 in 0.02 M Tris-HCl (pH 8.0), exciting the samples at 5 nm increments from 350 to 500 nm, and monitoring emission in the range from 500 to 630 nm. The excitation spectrum for each mutant was created using the emission intensity at 510 nm at each excitation wavelength that was measured. The excitation spectra were corrected for the wavelength-dependent excitation source intensity in the following way. The measured excitation spectrum for wtGFPuv was compared to the published wtGFPuv excitation spectrum, and a set of wavelength-dependent scaling factors was determined such that multiplying the measured wtGFPuv spectrum by the vector of scaling factors gave a spectrum identical to the published excitation spectrum of GFPuv (*9*). For those excitation wavelengths not reported previously (>480 nm), linear extrapolation of scaling factors determined over the region between 450 and 480 nm was used to generate scaling factors from 485 to 500 nm. All excitation spectra of the GFPuv mutants were then corrected using these scaling factors.

Quantification of Mixtures Using Lifetime Imaging. To determine the utility of the lifetime mutants for multiple-probe fluorescence lifetime imaging, 10 μL drops of varying compositions (binary mixtures of GFP molecules with different lifetimes) were placed on a clear Petri dish and imaged as described above. For each protein used, 1 μL of each isolated protein in buffer was imaged, and the wtGFPuv sample was diluted 1:20 in 0.02 M Tris-HCl (pH 8.0) while the other samples were diluted so that their total fluorescence intensity was roughly equal to that of wtGFPuv. A 10 μL drop of each protein alone was then imaged; the total emission collected from each pure protein was measured, and the lifetime (τ) for each protein was determined by fitting to eq 1. The composition of the binary mixtures was determined experimentally by fitting the fluorescence decay curves to the function

$$I = A_1 e^{(-t/\tau_1)} + A_2 e^{(-t/\tau_2)} \quad (2)$$

The fluorescence lifetime of each component in the mixture (τ_n) was held constant at the value of τ determined for the pure component, and the initial guesses for A_1 and A_2 were both 0.5. The values determined for A_1 by a least-squares fit of eq 2 gave the fraction of each sample consisting of wtGFPuv. This was then compared to the expected A_1 which was calculated from the fraction of each protein added, their relative total fluorescence intensities, and the ratio of their fluorescence lifetimes by

$$A_1 = f_1\left(\frac{1}{r_I - r_I f_1 + f_1}\right)\left(\frac{r_\tau}{1 - f_1 + r_\tau f_1}\right) \quad (3)$$

where f_1 is the volume fraction of the stock sample of wtGFPuv added to the mixture, r_I is the ratio of the total fluorescence intensity of the mutant to that of wtGFPuv in the stock samples, and r_τ is the ratio of the mutant's lifetime to that of wtGFPuv.

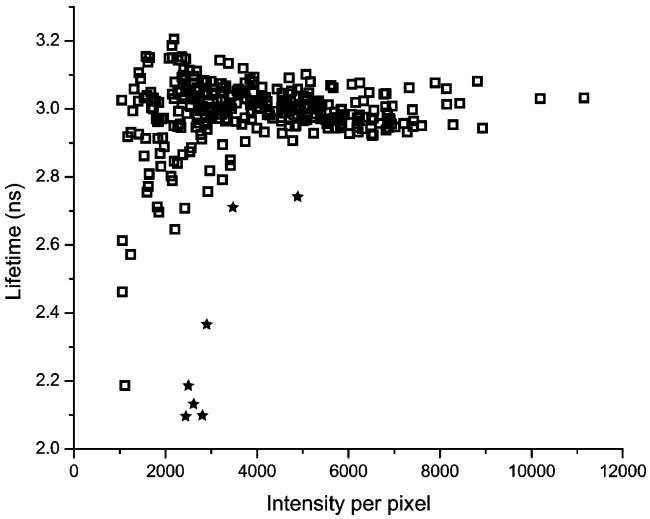

FIGURE 2: Fluorescence lifetime vs intensity per pixel for colonies in a first-generation GFPuv library. The apparent decrease in lifetime as the average intensity decreases is due to the increasing contribution from the plate media fluorescence which has a very fast decay time. Only colonies that exhibited a markedly decreased lifetime for a given intensity were selected for propagation to the next generation (selected colonies are represented by filled stars; remaining colonies are represented as empty squares).

RESULTS

Screening for Mutants with Altered Lifetimes. A typical plot of fluorescence lifetime versus average intensity for a first-generation library (containing ~10^4 total members) of GFPuv mutants is shown in Figure 2. As can be seen, there

Table 1: Representative Mutants and Lifetimes

	lifetime[a] (ns)	mutation(s)
wild type	3.03	–
mut1.3	2.78	Y145H
mut1.5	2.72	Y145H, V193A
mut1.9	2.74	Y145C
mut1.27	2.85	D103E, Y145H
mut1.28	2.76	S30R, Y145H
mut2.1	2.50	Y145H, V176A, N198I
mut2.2	1.94	S30R, Q69H, Y145H
mut3.3	1.88	S30R, F46L, Q69H, Y145H

[a] The standard deviation of all lifetime measurements is <0.075 ns.

is an apparent decrease in the fluorescence lifetime as the average intensity decreases, which is due to the increasing relative contribution of a short lifetime fluorescence component in the media to the overall intensity detected from the colony. Therefore, simply selecting colonies that have the shortest apparent lifetime is likely to yield mutants that only happen to fluoresce very poorly. By defining the selection criteria to choose colonies with a short lifetime for a given intensity, we can isolate mutations that affect the fluorescence lifetime, with the additional benefit being a minimal sacrifice of the fluorescence intensity of GFPuv. Therefore, only colonies that deviated significantly from the bulk of the population by appearing below and to the right of the curve were considered for selection.

The frequency of mutants with substantially altered lifetimes was found to be roughly 1 in every 1000 colonies screened. Using the sum of the decay from all pixels in a given colony required that the majority of fluorescent colonies be spatially separated from one another. Therefore, the density of the plates screened was typically ~100 colonies/cm^2, and the average colony size was ~500 μm. Using higher-density plates would have resulted in a substantial number of colonies growing in contact with one another, leading to an averaging of the lifetimes between multiple colonies. However, at the PCR error rate that was used (see Materials and Methods), one to three mutant colonies with altered lifetimes were found per plate. It is also interesting to note that no mutants exhibiting a lifetime longer than that of wtGFPuv were found during the screening process. Two mutants appearing to have longer lifetimes were selected in the first generation, but once the mutants were replated, their lifetime distribution was indistinguishable from that of wtGFPuv. The lack of mutants displaying a longer lifetime may be due to a lower frequency of these mutations, or it may be indicative that the quantum yield of wtGFPuv [0.79 (*13*)] is already at or near its maximum as a result of the combination of natural and in vitro evolutionary pressures to which it has been subjected (*9*).

Isolated Mutants. Table 1 lists all unique mutants isolated through three generations of selection, along with the fluorescence lifetime of each mutant expressed in *Escherichia coli* DH10B. As can be seen, all mutants contained a change at Y145, and in all but one, the tyrosine was mutated to histidine. The overall mean lifetime of the first-generation mutants when expressed in colonies was found to be 2.77 ± 0.05 ns, compared to a value of 3.03 ± 0.03 ns found for wtGFPuv. The lifetime versus intensity profiles of colonies expressing wtGFPuv and three mutants are plotted in Figure

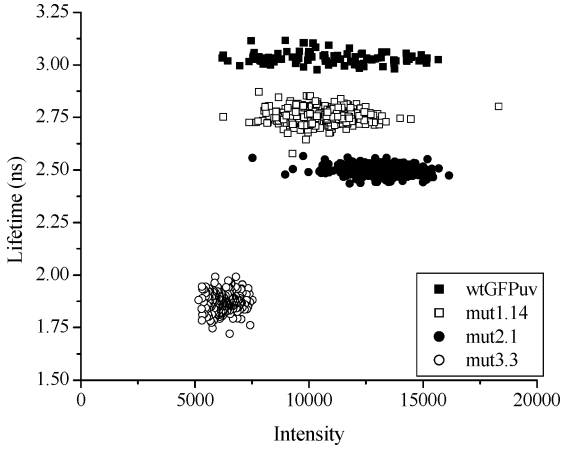

FIGURE 3: Lifetime vs intensity per pixel for colonies expressing wtGFPuv and three mutants. The mutants display high intensity and clearly distinct lifetimes.

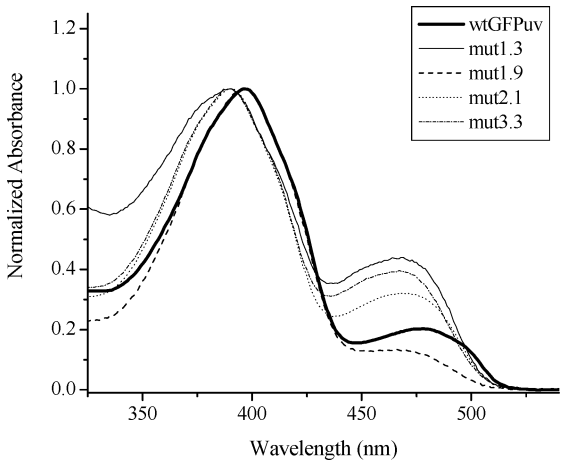

FIGURE 4: Normalized absorbance spectra of wtGFPuv and representative mutants. Each spectrum is normalized to its maximum. Mut1.3, mut2.1, and mut3.3 all exhibit a decrease in the ratio of absorbance at 400 nm to absorbance at 475 nm, accompanied by a blue shift of the 396 nm peak to ~390 nm, and a shift of the 478 nm peak to ~468 nm. Mut1.9 exhibits a relative increase in the ratio of absorbance at 400 nm to absorbance at 475 nm, and no blue shift in the 396 nm peak.

3, showing that the intensity per pixel for the first-generation mutant (mut1.14, Y145H) falls in the same range as that of wtGFPuv while having a clearly different lifetime. When selection was continued through the second and third generations, the Y145H mutation persisted in each of the isolated mutants, and the additional mutations S30R, Q69H, and F46L were found in combination with Y145H. As seen in Figure 3, the mutants all have fluorescence intensities comparable to that of wtGFPuv, while displaying distinct fluorescence lifetimes, which makes them ideal for differentiation in multiple-probe fluorescence lifetime imaging applications. Absorbance spectra of wtGFPuv and representative mutants are shown in Figure 4, and show that mutants containing a Y145H mutation (mut1.3, mut2.1, and mut3.3) show an increase in the 475 nm absorbance relative to the 396 nm peak, and a blue shift of each peak. The Y145C mutant (mut1.9) shows a decrease in the 475 nm absorbance relative to the 396 nm absorbance, and no blue shift in the 396 nm peak is present. Table 2 shows the absorbance maxima and A_{400}/A_{475} for each unique mutant. Fluorescence emission spectra of wtGFPuv and representative mutants

Table 2: Fluorescence Characteristics of wtGFPuv and Mutants

	absorbance maximum (nm)			excitation maximum (nm)		emission maximum (nm)	
	neutral	anion	A_{400}/A_{475}	neutral	anion	neutral[a]	anion[b]
wild type	396.0	478.0	4.92	400	480	508.4	505.7
mut1.3	390.0	469.0	2.27	400	480	507.7	503.3
mut1.5	390.0	468.0	2.29	395	480	506.4	503.1
mut1.9	397.0	466.0	7.17	400	480	509.7	503.5
mut1.27	390.0	469.9	2.29	395	465	506.8	503.8
mut1.28	390.0	468.0	2.62	390	480	506.2	502.9
mut2.1	391.0	468.0	3.12	390	480	507.1	504.2
mut2.2	389.0	466.0	2.68	395	465	507.9	504.4
mut3.3	390.0	467.0	2.52	390	465	506.2	504.0

[a] $\lambda_{ex} = 400$ nm. [b] $\lambda_{ex} = 480$ nm.

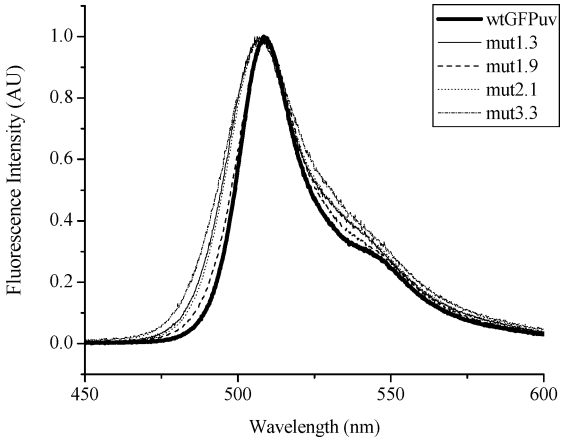

FIGURE 5: Fluorescence emission spectra of wtGFPuv and four mutants. Spectra were recorded with excitation at 400 nm. Mutant spectra show a slight blue shift in the emission maximum and broadening of the spectrum.

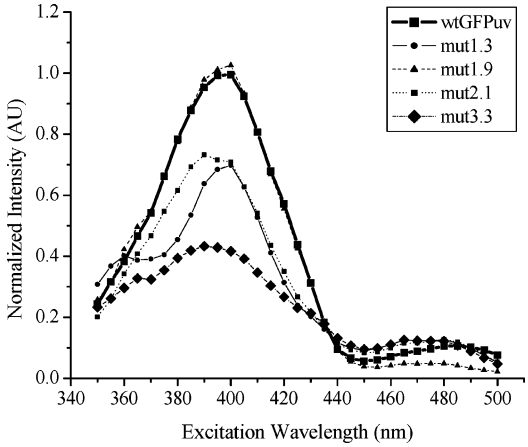

FIGURE 6: Excitation spectra of selected mutants with emission monitored at 510 nm. Spectra are corrected for lamp intensity as described in Materials and Methods.

measured using 400 nm excitation are shown in Figure 5. Mut1.3, mut2.1, and mut3.3, which all contain a Y145H mutation, display a 2 nm shift in their emission maximum relative to that of wtGFPuv. The spectrum of each mutant is also broadened relative to that of wtGFPuv. Excitation spectra of representative mutants with emission monitored at 510 nm are shown in Figure 6, and Table 2 gives the positions of the corresponding absorbance and excitation peaks for each mutant. Mut1.3 shows a large red shift in its excitation spectrum relative to the corresponding absorbance spectrum for both the neutral and anionic form of the chromophore. Mut1.9, mut1.28, and mut2.1 show similarly large red shifts of the excitation maximum of the anionic form of the chromophore relative to their maximal absorbance wavelengths, but not of the neutral form. Mut3.3 shows little such shift within the resolution of the measurement.

Table 3: Lifetimes of Isolated GFPuv and Mutants in Buffer

	lifetime[a] (ns)		lifetime[a] (ns)
wtGFPuv	3.39	mut2.1	2.87
mut1.3	3.04	mut3.3	2.12

[a] Lifetimes given as measured in 0.02 M Tris-HCl (pH 8.0).

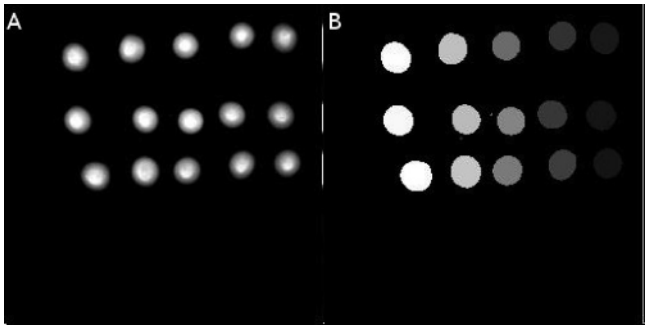

FIGURE 7: Analysis of binary mixtures of wtGFPuv and lifetime mutants. (A) Intensity image of 10 μL drops of binary mixtures of wtGFPuv and mut3.3. From left to right, each column consists of 95% wt GFPuv and 5% mut3.3, 75% wt GFPuv and 25% mut3.3, 50% wt GFPuv and 50% mut3.3, 25% wt GFPuv and 75% mut3.3, and 5% wt GFPuv and 95% mut3.3. (B) Image showing calculated A_1 values of each spot when decay curves derived from panel A were fit to eq 2. The decreasing content of wtGFPuv moving from left to right is clear.

Imaging of Isolated Mutants. The library of mutants isolated in these experiments should prove to be useful in multiprobe lifetime imaging. To demonstrate their utility in such imaging applications, the combination of wtGFPuv with selected mutants in different compositions was imaged and analyzed according to eq 2. For these fits, the fluorescence lifetimes were fixed on the basis of measurements of the individual proteins in isolation. Imaging 10 μL drops of wtGFPuv and three of the mutants separately yielded lifetimes given in Table 3. Binary wtGFPuv/mutant mixtures consisting of 5 and 95%, 25 and 75%, 50 and 50%, 75 and 25%, or 95 and 5% of each, respectively, were made, and 10 μL drops of these mixtures were analyzed for composition by fitting to eq 2, holding τ_1 and τ_2 to the values given in Table 3 (the fractions of each mutant were set on the basis of the total fluorescence, not the actual concentration, as described in Materials and Methods). Figure 7a shows an intensity image of an array of mixtures (total GFP fluorescence), the left-most column being a mixture of 9.5 μL of a wtGFPuv sample and 0.5 μL of a mut3.3 sample and the right-most column being the inverse. Figure 7b shows an image of the fraction of wtGFPuv in each spot determined from a nonlinear least-squares analysis of the measured lifetimes (see Materials and Methods). As can be seen, although each spot is similarly bright in terms of total fluorescence, the relative contribution of the wtGFPuv lifetime component to the fluorescence from the drop decreases from left to right. A plot of the experimental versus theoretical fraction of each protein in the mixture (Figure 8) results in good agreement between the two, showing the ability to measure the relative amounts of each species by

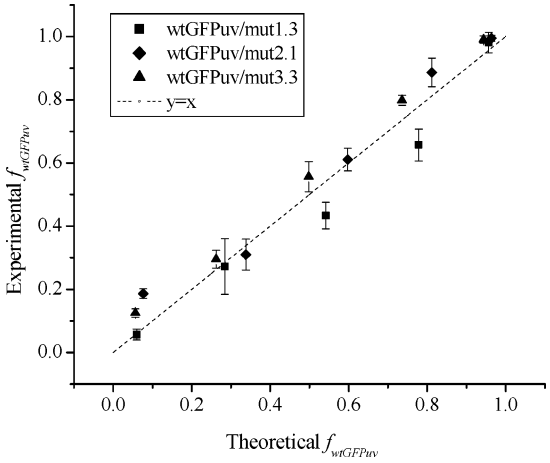

FIGURE 8: Plot of the experimentally determined fraction of wtGFPuv in binary mixtures with selected mutants vs the actual fraction in the drops. Error bars represent the standard deviation of three different drops for each condition that was measured. Good agreement is seen in the calculated relative composition and the experimentally determined compositions for each mutant, showing the ability to quantify each species in a mixture using only one detector channel.

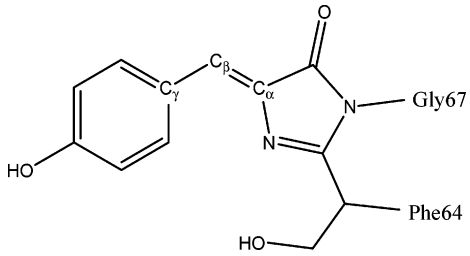

FIGURE 9: Schematic structure of the chromophore of GFP (adapted from ref *27*).

lifetime imaging in multiprobe experiments, provided the lifetimes of each are measured individually.

DISCUSSION

The fluorescent chromophore in GFP is formed autocatalyically from a Ser-Tyr-Gly peptide comprising residues 65−67 of the protein, and its final structure is shown in Figure 9 (*14*). This chromophore can exist in either the neutral form as shown or an anionic form in which the tyrosyl hydroxyl is deprotonated. These two forms of the chromophore exhibit distinct absorbance and emission characteristics. Absorbance at 395 nm excites the neutral chromophore, which is rapidly deprotonated and fluoresces at 510 nm with a lifetime of 3.3 ns (*15*, *16*). The anionic form absorbs maximally at 475 nm, and emits at 508 nm with a lifetime of 2.8 ns (*15*, *16*).

Previous studies of GFP and its variants have found several mutations that alter the fluorescence decay time. Mutating Ser65 to Thr has been shown to change the wtGFP lifetime from 3.2 to 3.0 ns (*7*), and further incorporation of an F64L mutation (to form EGFP) results in a lifetime of ~2.8 ns (*7*, *17*). These results agree with quantum yield measurements for these mutants which show slight decreases in the quantum yields of S65T and EGFP (0.64 and 0.60, respectively) compared to that of wtGFP (quantum yield of 0.79) (*13*, *16*). The mutants F64L/S65T/T203Y and F64L/S65T/Y145F/H148V/V150A/I167V were found to have average lifetimes of fluorescence of 0.3 and 0.5 ns at 515 nm when excited at 400 nm (*18*). This was attributed to an increase in the rate of internal conversion, because of an increase in the conformational degrees of freedom. The triple mutant F64M/S65G/Q69L was found to have a major lifetime component of 1.1 ns, which was attributed to the increased flexibility introduced by the S65G mutation and the disruption of the hydrogen bonding network around the chromophore by the Q69L mutation (*19*).

Some mutants of cyan fluorescent protein (CFP) and yellow fluorescent protein (YFP) have been found to increase the fluorescence decay lifetime. Enhanced CFP (ECFP) has been shown to decay biexponentially with a 3.6 ns component (0.86) and a 1.2 ns component [0.12 (*8*)]. In ECFP, the H148D mutation was found to result in a decay that was best described by a single 3.6 ns component, and the further inclusion of S72A and Y145A mutations was found to result in a fluorescence decay time of 3.3 ns. In a comparative study of different GFP mutants by Pepperkok et al. (*5*), they determined lifetimes of 2.59 ns for the S65T mutant of GFP and 2.42 ns for EGFP, while the mutant designated YFP5, with nine total mutations relative to wtGFP, had a lifetime of 3.60 ns. While these mutants show an increase in lifetime, the mechanisms behind these changes are not known in any detail.

Decay Pathways in Model Chromophore Compounds. A recent study of a GFP-chromophore model compound in solutions of varying viscosities at different temperatures revealed that while no fluorescence was seen at room temperature in ethanol, measurements at 100 K revealed longer-lived fluorescence (*20*). In glycerol at 150 K, the neutral chromophore compound had a monoexponential decay of 2.1 ns, while the anionic form displayed a single-exponential 3.0 ns decay. While both forms of the chromophore can decay by either $C_\beta-C_\gamma$ bond rotation or by $C_\beta-C_\alpha$ bond rotation, the neutral chromophore predominantly decays by $C_\beta-C_\gamma$ bond rotation, while $C_\beta-C_\alpha$ bond rotation is the more energetically favorable decay pathway for the anionic form (*20*). Both of these rotations are similarly allowed for model chromophores in solution, whereas $C_\beta-C_\alpha$ bond rotation is sterically suppressed by the protein environment in GFP. These interpretations are supported by recent molecular mechanics simulations of the chromophore cavity of the protein (*21*) and structural simulations of a model chromophore in vacuo (*22*), which both suggest that rotation around the $C_\beta-C_\gamma$ bond is likely to be the main nonradiative relaxation pathway of the GFP chromophore excited states.

Implications for Isolated Mutants. GFPuv, the fluorescent protein platform used to generate these mutants, has three amino acid substitutions relative to wtGFP [F99S/M153T/V163A (*9*)]. The crystal structure of GFPuv shows that all three mutations are present on the surface of the β-can, and have little impact on the structural configuration of the chromophore (*23*). There is a good agreement between the fluorescence lifetime of GFPuv measured in this study and those reported previously for wtGFP (*16*). Measurements of the quantum yield of GFPuv have shown it to be close to that of wtGFP as well (*13*). While the spectral analysis of the mutants isolated here, particularly those involving Y145H, shows distinct blue shifts in absorbance and emission, as well as a clear shift in the ground state equilibrium between the neutral and ionic forms relative to wtGFPuv, these changes are likely not correlated to the changes in the

excited state lifetimes determined here. There is no simple relationship between the magnitude of the blue shifts caused by the mutations or the relative ratios of absorbance at 400 nm to absorbance at 475 nm and the magnitudes by which the lifetimes are altered in each mutant. In fact, in the Y145C mutant, the ground state equilibrium between the neutral and anionic forms is shifted in the opposite direction from the Y145H mutants, yet a decrease in the fluorescence lifetime is seen comparable to that for the single Y145H mutation. One common feature seen in the first-generation mutants is a red shift in the peaks of their excitation spectra relative to their absorbance spectra. This, coupled with the blue shift in the absorbance spectra relative to that of wtGFPuv, indicates that the predominant absorbing states of the chromophore in the first-generation mutants are weakly fluorescent states that are not accessible in wtGFPuv. These states likely have a much shorter fluorescence lifetime than the lifetime of wtGFPuv, leading to the shorter observed fluorescence lifetimes in these mutants. Both the neutral and the anionic form show this red shift between absorbance and excitation spectra, although it is more pronounced for the anionic form.

The first-generation mutants have a mutation at Y145 in common, and this apparently leads to an increase in the flexibility of the protein, allowing the chromophore to exist in a wider range of conformational states. This interpretation is supported by the crystal structure of wtGFPuv, which shows that Y145 is in van der Waals contact with the phenolic end of the chromophore and may sterically restrict movement of this part of the chromophore (*23*). The phenolic ring of Y145 is also packed against the side chains of several amino acids, some of which are in direct contact with the chromophore. Kummer et al. (*18*) found that the excited state lifetime was shortened for a GFP variant containing the Y145W mutation, possibly due to a rearrangement of packing interactions in response to the bulky nature of the introduced tryptophan. In mutants in which the chromophore-forming tyrosine residue is substituted with either a histidine (blue fluorescent protein, BFP, Y66H) or a tryptophan (cyan fluorescent protein, CFP, Y66W), mutations which appear to compensate for the change in chromophore size have been identified. In BFP, the additional Y145F substitution leads to a doubling of the quantum yield (*24*). In this variant, a backbone shift around His148 toward the protein interior likely compensates for structural perturbations that result from the less bulky chromophore (*25*), suggesting that replacement of Y145 with a phenylalanine is important in rearranging the interior architecture. In CFP, the Y145G or Y145A mutation likely acts as a compensating mutation that improves packing interactions around the very bulky chromophore, which, in combination with other mutations, results in a variant with improved FRET (*8*). In analogy to the above examples, the Y145H or Y145C substitution isolated in GFPuv likely results in an uncompensated perturbation of the interior architecture around the phenolic end of the chromophore, and this could allow a wider range of conformations to be adopted by the chromophore. In this case, the excited state probably undergoes internal conversion by $C_\beta-C_\gamma$ bond rotation more rapidly, leading to a shorter fluorescence lifetime.

In the second generation, introduction of the V176A and N198I mutants into the Y145H mutant results in a decrease in the lifetime to 2.5 ± 0.02 ns, while the red shift of the excitation spectrum relative to the absorbance spectrum for the neutral form of the chromophore is nearly eliminated. Thus, these mutations may stabilize the short lifetime conformations of the chromophore, leading to the shorter average lifetime observed for mut2.1. Mut2.2, with S30R and Q69H mutations in addition to Y145H, showed a fluorescence lifetime of 1.94 ± 0.04 ns, and exhibited the largest blue shift of the neutral chromophore absorbance relative to wtGFPuv. Q69 is intimately involved in the hydrogen bonding network, including Q94 and R96, and also is in van der Waals contact with the chromophore's carbonyl group. Thus, it would seem that Q69H serves to further increase the flexibility of the protein environment of the chromophore relative to Y145H, resulting in an increased population of conformations with accelerated internal conversion rates, and an overall shorter average lifetime. By analogy with the observations of Volkmer et al. (*19*) that mutation of Q69 to leucine disrupts the hydrogen bond network surrounding the chromophore, resulting in a decreased fluorescence lifetime, the Q69H mutation probably acts through a similar mechanism.

The third-generation mutant mut3.3, which contains S30R, F46L, Q69H, and Y145H mutations, shows excitation spectra maxima at the same wavelengths as absorbance maxima (but both blue shifted relative to those of wtGFPuv), indicating that the predominant absorbing and emitting species are the same. F46L thus is likely to stabilize a short lifetime conformation of the chromophore which gives rise to the majority of fluorescence from this mutant. The structure of wtGFPuv shows that F46, which is approximately 8 Å from the chromophore, is π-stacked with F64, which is immediately adjacent to the chromophore in the primary amino acid sequence of wtGFPuv. F64 is also in contact with W57, forming a hydrophobic pocket in the interior of the protein along with several other hydrophobic residues (*23*). Replacing W57 with phenylalanine reduces the efficiency of autocatalytic chromophore formation, likely by disrupting the packing interactions that properly align residues involved in generating the chromophore (*26*). F64 has also been shown to be an important contributor to the flexibility of GFP (*18*).

While the interpretations of the effects of the particular amino acid substitutions found in this study remain speculative at present, the hypothesis that short lifetime conformations of the protein are populated more frequently in the mutants can be tested by measuring the lifetime as a function of excitation wavelength in wtGFPuv and mutants, with the expectation that excitation on the blue side of the absorbance peaks of the mutants would result in shorter fluorescence lifetimes than excitation on the red side, as the shorter lifetime conformations appear to be blue-shifted. Investigations of this nature are currently underway in our laboratory.

It is interesting to note that no mutations resulting in fluorescence lifetimes longer than wtGFPuv were isolated. This may be due to an inadequate mutant library size for detection of these mutations, which may occur at lower frequencies than mutations that decrease the lifetime. This rarity can be due to either library bias against such mutations or an inherent difficulty in increasing the natural radiative lifetime or quantum yield of GFPuv.

Lifetime mutants such as those isolated here hold great promise for the field of multiprobe in vivo fluorescence

imaging by providing both a set of GFP variants that can be resolved using a single-detector channel and a method for creating similar mutants derived from other fluorescent proteins with different colors. The ability to quantify the relative amounts of different mutants in solution based on lifetime imaging demonstrated here provides a basis for the future use of these mutants in multiprobe in vivo imaging experiments. Further, subjecting other fluorescent proteins to directed evolution to select for mutants with varied lifetimes would result in a library of fluorescent proteins that can be resolved on the basis of both spectral and lifetime differences. Detection of fluorescence using multiple spectral channels in a time-resolved way could then lead to the ability to discriminate and quantify an increased number of fluorescent protein-labeled species within a sample simultaneously. In addition, lifetime mutants such as these make it possible to image multiple fluorescent proteins in a cell without using an instrument containing wavelength separation optics. This could be very useful for situations in which very small footprint measuring equipment (such as a microfluidic system) is required. Overall, the expansion of the number of resolvable fluorescent proteins should lend itself favorably to a wide range of imaging applications in biology.

REFERENCES

1. Duncan, R. R., Bergmann, A., Cousin, M. A., Apps, D. K., and Shipston, M. J. (2004) Multi-dimensional time-correlated single photon counting (TCSPC) fluorescence lifetime imaging microscopy (FLIM) to detect FRET in cells, *J. Microsc. (Oxford, U.K.) 215*, 1−12.
2. Hailey, D. W., Davis, T. N., and Muller, E. G. D. (2002) Fluorescence resonance energy transfer using color variants of green fluorescent protein, in *Guide to Yeast Genetics and Molecular and Cell Biology*, Part C, pp 34−49, Academic Press, San Diego.
3. Lansford, R., Bearman, G., and Fraser, S. E. (2001) Resolution of multiple green fluorescent protein color variants and dyes using two-photon microscopy and imaging spectroscopy, *J. Biomed. Opt. 6*, 311−318.
4. Lippincott-Schwartz, J., and Patterson, G. H. (2003) Development and use of fluorescent protein markers in living cells, *Science 300*, 87−91.
5. Pepperkok, R., Squire, A., Geley, S., and Bastiaens, P. I. H. (1999) Simultaneous detection of multiple green fluorescent proteins in live cells by fluorescence lifetime imaging microscopy, *Curr. Biol. 9*, 269−272.
6. Zimmermann, T., Rietdorf, J., and Pepperkok, R. (2003) Spectral imaging and its applications in live cell microscopy, *FEBS Lett. 546*, 87−92.
7. Heikal, A. A., Hess, S. T., and Webb, W. W. (2001) Multiphoton molecular spectroscopy and excited-state dynamics of enhanced green fluorescent protein (EGFP): Acid−base specificity, *Chem. Phys. 274*, 37−55.
8. Rizzo, M. A., Springer, G. H., Granada, B., and Piston, D. W. (2004) An improved cyan fluorescent protein variant useful for FRET, *Nat. Biotechnol. 22*, 445−449.
9. Crameri, A., Whitehorn, E. A., Tate, E., and Stemmer, W. P. C. (1996) Improved green fluorescent protein by molecular evolution using DNA shuffling, *Nat. Biotechnol. 14*, 315−319.
10. Doi, N., and Yanagawa, H. (1999) Design of generic biosensors based on green fluorescent proteins with allosteric sites by directed evolution, *FEBS Lett. 453*, 305−307.
11. Leung, D. W., Chen, E., and Goeddel, D. V. (1989) A method for random mutagenesis of a defined DNA segment using a modified polymerase chain reaction, *Technique 1*, 11−15.
12. Katiliene, Z., Katilius, E., Uyeda, G. H., Williams, J. C., and Woodbury, N. W. (2004) Increasing the rate of energy transfer between the LHI antenna and the reaction center in the photosynthetic bacterium *Rhodobacter sphaeroides*, *J. Phys. Chem. B 108*, 3863−3870.
13. Patterson, G. H., Knobel, S. M., Sharif, W. D., Kain, S. R., and Piston, D. W. (1997) Use of the green fluorescent protein and its mutants in quantitative fluorescence microscopy, *Biophys. J. 73*, 2782−2790.
14. Cody, C. W., Prasher, D. C., Westler, W. M., Prendergast, F. G., and Ward, W. W. (1993) Chemical structure of the hexapeptide chromophore of the *Aequorea* green-fluorescent protein, *Biochemistry 32*, 1212−1218.
15. Chattoraj, M., King, B. A., Bublitz, G. U., and Boxer, S. G. (1996) Ultra-fast excited-state dynamics in green fluorescent protein: Multiple states and proton transfer, *Proc. Natl. Acad. Sci. U.S.A. 93*, 8362−8367.
16. Striker, G., Subramaniam, V., Seidel, C. A. M., and Volkmer, A. (1999) Photochromicity and fluorescence lifetimes of green fluorescent protein, *J. Phys. Chem. B 103*, 8612−8617.
17. Cotlet, M., Hofkens, J., Maus, M., Gensch, T., Van der Auweraer, M., Michiels, J., Dirix, G., Van Guyse, M., Vanderleyden, J., Visser, A., and De Schryver, F. C. (2001) Excited-state dynamics in the enhanced green fluorescent protein mutant probed by picosecond time-resolved single photon counting spectroscopy, *J. Phys. Chem. B 105*, 4999−5006.
18. Kummer, A. D., Kompa, C., Lossau, H., Pollinger-Dammer, F., Michel-Beyerle, M. E., Silva, C. M., Bylina, E. J., Coleman, W. J., Yang, M. M., and Youvan, D. C. (1998) Dramatic reduction in fluorescence quantum yield in mutants of green fluorescent protein due to fast internal conversion, *Chem. Phys. 237*, 183−193.
19. Volkmer, A., Subramaniam, V., Birch, D. J. S., and Jovin, T. M. (2000) One- and two-photon excited fluorescence lifetimes and anisotropy decays of green fluorescent proteins, *Biophys. J. 78*, 1589−1598.
20. Kummer, A. D., Kompa, C., Niwa, H., Hirano, T., Kojima, S., and Michel-Beyerle, M. E. (2002) Viscosity-dependent fluorescence decay of the GFP chromophore in solution due to fast internal conversion, *J. Phys. Chem. B 106*, 7554−7559.
21. Baffour-Awuah, N. Y. A., and Zimmer, M. (2004) Hula-twisting in green fluorescent protein, *Chem. Phys. 303*, 7−11.
22. Martin, M. E., Negri, F., and Olivucci, M. (2004) Origin, nature, and fate of the fluorescent state of the green fluorescent protein chromophore at the CASPT2//CASSCF resolution, *J. Am. Chem. Soc. 126*, 5452−5464.
23. Battistutta, R., Negro, A., and Zanotti, G. (2000) Crystal structure and refolding properties of the mutant F99S/M153T/V163A of the green fluorescent protein, *Proteins 41*, 429−437.
24. Hein, R., and Tsien, R. Y. (1996) Engineering green fluorescent protein for improved brightness, longer wavelengths and fluorescence resonance energy transfer, *Curr. Biol. 6*, 178−182.
25. Wachter, R. M., King, B. A., Heim, R., Kallio, K., Tsien, R. Y., Boxer, S. G., and Remington, S. J. (1997) Crystal structure and photodynamic behavior of the blue emission variant Y66H/Y145F of green fluorescent protein, *Biochemistry 36*, 9759−9765.
26. Bell, A. F., Stoner-Ma, D., Wachter, R. M., and Tonge, P. J. (2003) Light-driven decarboxylation of wild-type green fluorescent protein, *J. Am. Chem. Soc. 125*, 6919−6926.
27. Brejc, K., Sixma, T. K., Kitts, P. A., Kain, S. R., Tsien, R. Y., Ormo, M., and Remington, S. J. (1997) Structural basis for dual excitation and photoisomerization of the *Aequorea victoria* green fluorescent protein, *Proc. Natl. Acad. Sci. U.S.A. 94*, 2306−2311.

BI050550F